Journal of Applied Sciences

ISSN 1812-5654

science alert

ANSInet
an open access publisher
http://ansinet.com

Journal of Applied Sciences 11 (10): 1784-1790, 2011
ISSN 1812-5654 / DOI: 10.3923/jas.2011.1784.1790

Machining of Cemented Tungsten Carbide using EDM

A.T.Z. Mahamat, A.M.A. Rani and Patthi Husain
Department of Mechanical Engineering, Universiti Teknologi PETRONAS,
Bandar Seri Iskandar, 31750 Tronoh, Perak, Malaysia

Abstract: In this study, we investigate the possibility of machining cemented tungsten carbide WC+6% Co by using copper. Tungsten carbide is hard and brittle with low thermal conductivity and low thermal expansion. The high resistant to abrasive wear and high melting point are the main reason for the selection of these materials for large number of applications such as machining tool and die material. The hardness of WC+Co primarily depends on the average grain size and cobalt content. The difficulty when machining cemented tungsten carbide comes from the thermal stress. The micro cracks enlarge, which leads to macro crack and fragmentation. This can be referred to the low thermal expansion, thermal conductivity and brittleness, which create a high thermal stress. Generally, cooling and removal of the cracked particles are difficult. In order to develop the optimal machining process for the desirable machining response, L_9 Taguchi Orthogonal Array (OA) were used. This orthogonal array is used for optimization of the following variables; Peak-Current (IP), pulse ON-Time (ON), pulse OFF-Time (OFF) and Gap-Voltage (GAP). The results show that it's possible to EDMing WC-Co using copper electrode at very low energy setting but at the expense of material removal rate MRR.

Key words: Copper electrode, diesinker EDM, cemented tungsten carbide, taguchi DOE

INTRODUCTION

Cemented tungsten carbide mainly used as marching tools. The combination of a large percentage of Tungsten carbide ceramic particles with a small percentage of a metallic binder make this material have a properties neither of metal nor of ceramic (Upadhyasa, 1998). Since this material is electrically conductive, it is possible to be machined into complex forms by the Electrical Discharge Machining. Other possible machining technique for this material is the water jet (Khan *et al*., 2005).

This material has a high wear resistant due to its high hardness value of 1500 Vickers and good dimensional stability. These properties make the material suitable for gage applications. The very low thermal expansion and the low thermal conductivity in combination with high melting point and brittleness are the main source of machining difficulties.

Seghouani *et al*. (2010) study the demanding of cutting tool rather than carbide During the Turning of not Hardened Steel XC38. He show that it possible to determine the time of change of the tool and to regard it as constraint for the respect of the roughness of the work piece during a work of series in conventional machining (Jahan *et al*., 2009).

In his study, found that the surface characteristics are dependent mostly on the discharge energy during machining. In addition, the surface finish was found to be influenced greatly by the electrical and thermal properties of the electrode material. It was found that Ag-W electrode produces smooth surface. On the other hand, Cu-W electrodes achieved the highest MRR followed by Ag-W. In the case of electrode wear, the W electrode has the lowest wear followed by copper-tungsten and silver-tungsten.

Rahman *et al*. (2011) investigated the machining characteristics of austenitic stainless steel 304 through electric discharge machining. The effectiveness of the EDM process with stainless steel is evaluated in terms of the removal rate (MRR), the Tool Wear Rate (TWR) and the surface roughness of the work-piece produced. The experimental work is conducted utilizing Die Sinking EDM using copper electrode. From the experimental results no tool wear condition is noted for copper electrode at long pulse-on time with reverse polarity. The optimal pulse-on time is changed with high ampere.

Lee and Li (2003) found that there is no difference between the hardness of the EDM surface and the original hardness of workpiece at all EDM conditions. It is observed from the SEM micrographs that there is a clear

Corresponding Author: A.T.Z. Mahamat, Department of Mechanical Engineering, Universiti Teknologi PETRONAS, Bandar Seri Iskandar, 31750 Tronoh, Perak, Malaysia

EDM damaged layer on the workpiece, distinguished by the amount of WC grains and micro-cracks. It is observed that the depth of the damaged layer and number of micro-cracks increase with the Peak-Current and pulse duration.

Puertas *et al.* (2004) found that in the case of the Ra parameter the most influential factors is the intensity, followed by the pulse time factor, while the duty cycle factor was not significant. In the case of electrode wear, it was also seen that the intensity factor was the most influential.

Luis *et al.* (2005) study the Material Removal Rate (MRR) and Electrode Wear (EW) on the die-sinking EDM of reaction-bonded silicon carbide. He concludes that In the case of MRR, the only influential design factors were: intensity and voltage. For EW the most important variables are: intensity, pulse time and flushing pressure.

MATERIALS AND METHODS

The workpiece specimen is prepared from tungsten carbide rod (YG6) with 50 mm diameter and 100 mm high. It`s divided cross-sectional into nine equal disc using wire cut EDM. The pieces sectioned and divided into four equal specimens. The electrodes were manufactured from a 20×20 mm copper bar into a hallow cylinder of 5mm internal diameter and 13mm diameters external diameter. The main electrode and workpiece properties are shown in Table 1.

The experimental work was conducted on Mitsubishi EA series oil die sinking EDM machine. The machining variables and their levels are shown in Table 2 where the other variables kept constant.

The L_9 taguchi orthogonal array experimental layout and the observed values of the machining output (responses) are shown in Table 3. The mean averages of responses are indicated in Table 4. By L_9 taguchi orthogonal array, we use relatively few experiment.

The material removal rate MRR and electrode wear EW were measured as mass different/machining time in (g min^{-1}) and the tool wear ratio TWR measured as the percentage ratio of (EW/MRR). The surface roughness SR was measured by using Mitutoyo surface roughness tester by taking the average of 10 readings at different lines parallel to the axis of the machined cylinder.

For further investigation optical microscopy SEM and EDX were taken. The effect of machining condition on metallurgical and surface morphology is significant. The inspected areas were selected at the edge of the machined surface.

Data analyzed using analysis of variance (ANOVA) and Eq. 1, 2 and 3 to indicate the impact of process parameters on process response (Yang *et al.*, 2009).

$$SS = \frac{k}{N*n}\sum_{i=1}^{k} T_i^2 - \frac{T_t^2}{N*n} \quad (1)$$

$$SS_t = SS_{IP} + SS_{ON} + SS_{OFF} + SS_{GAP} + S_{error} \quad (2)$$

Table 1: The main electrode and workpiece properties

	Composition	Thermal conductivity (W m^{-1} K^{-1}) at 38°C	Electrical conductivity (%IACS)	Melting point (°C)
Copper electrode	100% Cu	385	90-100	1084
WC-Co workpiece	WC-94%, Co-6%	45-80	7.5-12	2800
	Heat capacity J mol^{-1} K^{-1}	Hardness HV	Density (g cm^{-3})	Thermal expansion 10^{-6} ($°C^{-1}$)
Copper electrode	24	369	8.9	17
WC-Co workpiece	2.8	1660	14.6	4.9×10-4

Table 2: Machining variables and their levels

Levels	Peak-current notch (Amp)	Pulse on-time notch (μ-second)	Pulse off-time notch (μ-second)	Gap-voltage notch (volt)
1	3.2 [12]	6 [64]	4 [16]	10 [80]
2	3.4 [14]	7 [128]	5 [32]	11 [110]
3	3.5 [15]	8 [256]	6 [64]	12 [150]

Table 3: L9 Taguchi orthogonal array with the four machining responses

Exp.No.	Peak-current	Pulse on-time	Pulse off-time	Gap-voltage	MRR (g min^{-1})	EW (g min^{-1})	TWR (%)	SR
1	3.2	6	4	10	0.0038	0.0007	0.183	6.8
2	3.2	7	5	11	0.0061	0.0012	0.194	2.9
3	3.2	8	6	12	0.0061	0.0014	0.230	3.1
4	3.4	6	5	12	0.0062	0.0015	0.244	5.9
5	3.4	7	6	10	0.0043	0.0010	0.224	3.3
6	3.4	8	4	11	0.0048	0.0013	0.268	3.7
7	3.5	6	6	11	0.0025	0.0004	0.156	11.8
8	3.5	7	4	12	0.0030	0.0005	0.177	4.7
9	3.5	8	5	10	0.0056	0.0013	0.238	3.8

Table 4: Mean averages of responses

	Variables level	Peak current	Pulse on-time	Pulse off-time	Gap voltage
MRR mean Response	1	0.005328	0.004171	0.003826	0.004547
	2	0.005082	0.004442	0.005982	0.004466
	3	0.003695	0.005493	0.004298	0.005092
EW mean Response	1	0.001096	0.000870	0.000831	0.000996
	2	0.001253	3.467	0.001352	0.000954
	3	0.000753	0.001341	0.000920	0.001152
TWR mean Response	1	0.2029	0.1948	6.067	0.2156
	2	6.700	0.1992	0.2262	0.2065
	3	0.1909	8.167	0.2038	6.133
SR mean Response	1	4.267	3.633	5.067	4.567
	2	4.300	0.2458	4.133	4.567
	3	0.2460	0.000892	0.2099	0.2177

$$\frac{SS_{IP}}{SS_t}+\frac{SS_{ON}}{SS_t}+\frac{SS_{OFF}}{SS_t}+\frac{SS_{GAP}}{SS_t}+\frac{SS_{error}}{SS_t}=100\% \qquad (3)$$

where, SS is the sum square, SS the total sum of the square and $\frac{SS_i}{SS_t}$ is the percentage effect of each variable. K is the parameters levels; N is the total number of run; n the number of replication; T_i is the total sum of response at i_{th} level and T_t is the total sum of responses.

RESULTS AND DISCUSSION

Material removal rate: The variables Percentage Contribution on MRR calculated from Table 4 using Eq. 1, 2 and 3 shown in Fig. 1 and 2. It's clear that the most effective variables on the MRR are pulse OFF-Time and pulse ON-Time respectively. The Peak-Current and the Gap-Voltage have a total contribution of less than 18%. The main-effects chart of Fig. 3 indicates that for optimal MRR, pulse ON-Time and Gap-Voltage setting should be set at level 3, the Peak-Current should be at least 1 and pulse OFF-Time at level 2. But During the experiment we noted that in order to get normal machining process, the Gap-Voltage should be set at lower level less than 150 volt. Higher Gap-Voltage is the main source of crack initiation, cracks enlargement and fragmentation. The machining process highly affected by the fragmented particles. The effect includes thicker carbon layer on the electrode surface, massive bobble, random machining depth reading and even machine auto stop.

Other effective variable mentioned by Lonardo and Bruzzone (1999) includes flushing mode and electrode type. The observed results show the importance of electrode material, injection flushing and geometry on material removal rate, electrode wear and surface quality.

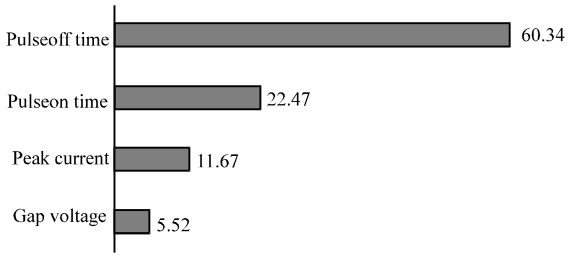

Fig. 1: Percentage contribution of variables on MRR

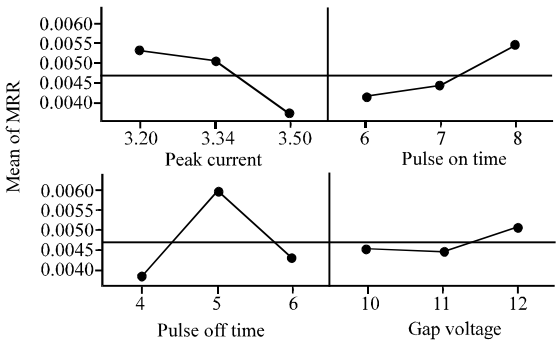

Fig. 2: Main effect chart of MRR

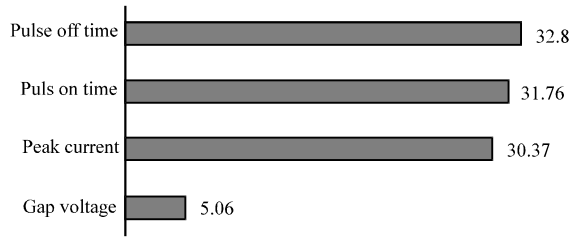

Fig. 3: Percentage contribution of variables on EW

Electrode wear: The percentage contribution of variables on the EW is different from MRR. Figure 4 show that pulse on OFF-Time, pulse ON-Time and Peak-Current are the most effective variables on EW. The effect of Gap-voltage on the electrode wear is negligible. The Gap-voltage is the main source thermal stress. Some of the fragmented particles implanted into the electrode surface and becomes as new electrode tips. After implantation, the discharge process continue between the new tip and the work piece and this can explain why the effect of Gap-

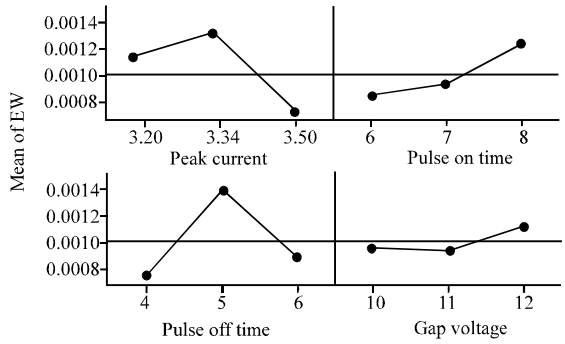

Fig. 4: Main effect chart of EW

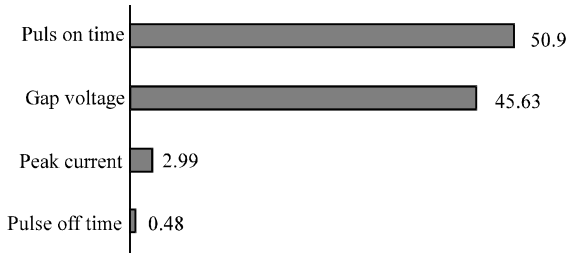

Fig. 5: Percentage contribution of variables on TWR

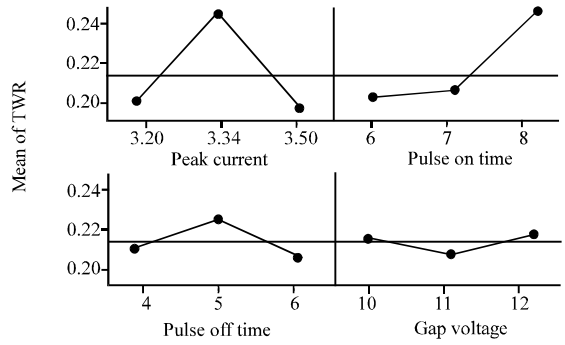

Fig. 6: Main effect chart of TWR

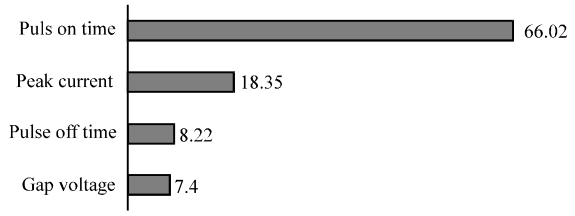

Fig. 7: Percentage contribution of variables on SR

Voltage are more clear on MRR than the electrode wear. Figures 5 shows the main effects of machining variables on the electrode wear. The reduction of electrode wear requires that; pulse ON-Time, pulse OFF-Time and the Gap-Voltage should be set at lower levels. Electrodes wear decreases as the Peak - Current increases. The effect of Peak-Current on the electrode wear rate requires more investigation taking into account the interaction of this variable with ON-Time, OFF-Time and Gap-Voltage.

Table 5: Expected prediction value at the optimal setting

	Peak-current amp	Pulse on-time [µsec]	Pulse off-time [µsec]	Gap-voltage [volt]	Predicted values of MRR, EW, TWR and SR
MRR	3.2	8	4	10	0.007243
EW	3.5	6	4	10	0.0003474
TWR	3.4	8	5	10	0.165370
SR	3.2	8	5	10	3.6

Tool wear ratio: Figures 6 is the percentage contribution of variables on tool wear ratio and Fig. 7 show the mean effects of variables on TWR. From Figure 6, the most important factors are pulse ON-Time and Gap-Voltage, respectively.

The Tool wear ratio increases when these two Factors increased. These can be expected as the increase in these variables means more discharge energy. From Fig. 7, Optimization of TWR Depends on the criterion lower TWR is best requires that; the Peak-Current, pulse on-time and pulse OFF-Time should set to high level. Meanwhile Gap-Voltages as mention should be set at lower level. A set of factor level combinations that can give minimum TWR are shown in prediction Table 5.

Surface roughness: Figure 8 shows that the values of the surface roughness highly effected by pulse ON-Time and Peak-Current respectively. Pulse ON-Time is significantly affective variable on all responses, but the highest contribution of this variable is on surface roughness. This can be referred to the effect of longer discharge time on heating and cooling rate and the number and size of the crater created. The increase of pulse ON-Time will affect the discharge efficiency, cooling rate and debris removal and as a consequence the surface roughness.

From Fig. 9, good surface roughness require low Peak-Current and high ON-Time. The Peak-Current is the most effective variable on the crater shape and the pulse ON-Time is highly effective on the crater size. Meanwhile the gap voltage is very effective on the number and size of the cracks. The measurement of surface roughness depends on these craters properties besides the surface crack and the fragmented particles. The predicted values of surface roughness and the equivalent Factor levels are shown in Table 5. Kiyak and Cakir (2007) found that surface roughness of workpiece and electrode were influenced by pulse current and pulse time, higher values of these parameters

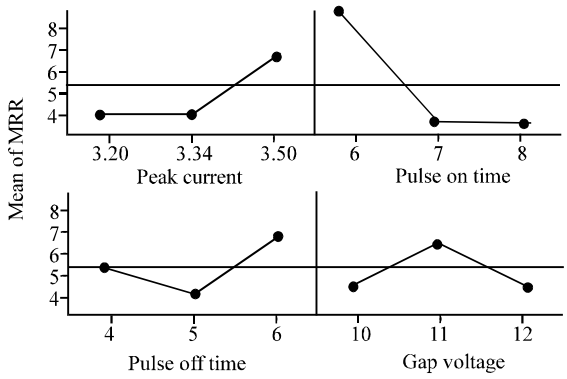

Fig. 8: Main effect chart of SR

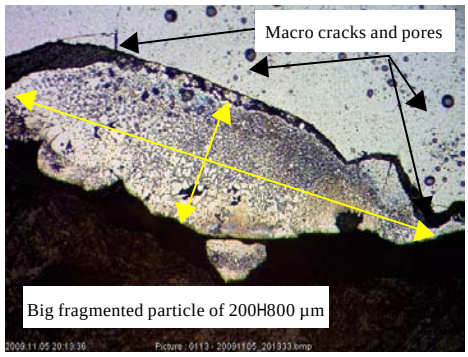

Fig. 11: Fractured part due to crack enlargement

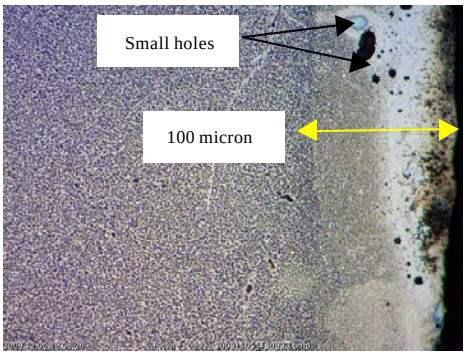

Fig. 9: Heat effected zone under low energy condition

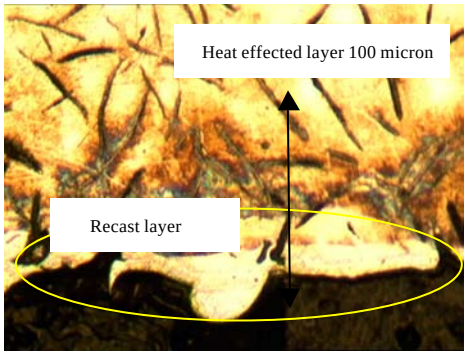

Fig. 12: Recast layer of machined gray cast iron

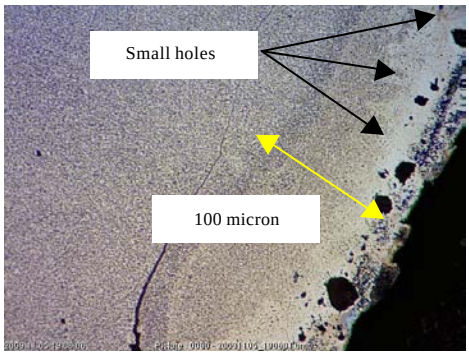

Fig. 10: Micro crack and holes due to high gap voltage

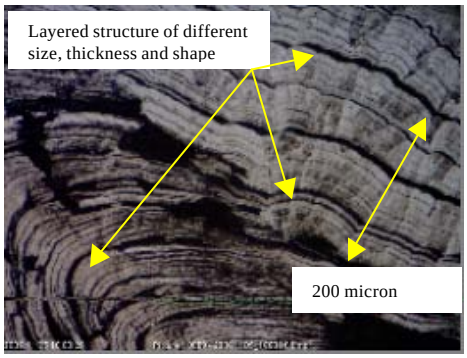

Fig. 13: Optical image of the accumulated solid material in the discharge gap

increased surface roughness. Lower current, lower pulse time and relatively higher pulse pause time produced a better surface finish.

Microstructure

Optical microscopic: Figure 9 shows the cress sectional optical images of the heat effected layer and Fig. 10 show the crack enlargement on the machined surface. Figure 12 shows that small particles are fragmented form the surface when machined at high gap voltage. Some particles fragmented from the workpiece left behind holes of different sizes. These fragmented particles dramatically have an effect on the machining process.

The cracks are generally initiated when the thermal stresses exceeding the ultimate tensile strength of the material. Low thermal conductivity, low thermal expansion, high heating rate and low cooling rate are the main causes

of the thermal stress. This thermal stress initiates a few micro cracks which enlarge to macro crack due to unbalanced heating and cooling rate.

Some of the cracks terminate within the white layer and the other enlarged and propagates hundreds of micron inside the machined surface. In addition, the number and the size of the cracks and holes depend mainly on the gap voltage. Xu *et al*. (2009) investigate the Material removal mechanisms of cemented carbides machined by ultrasonic vibration assisted EDM in gas medium. The mechanisms discussed in detail through observing and analyzing the microstructures of machined surface. Also (Ratnasingam *et al*., 2009) study the Wear Characteristics of Cemented Tungsten Carbide Tools in Machining Oil Palm Empty Fruit Bunch Particleboard. he was found that mechanical abrasion and micro-fracture was the primary mode of tool failure.

The comparison between Fig. 11 of the machined cemented tungsten carbide and Fig. 12 of gray cast iron show that the quality of the surface not only depends on the machining condition, but also depends on the workpiece and electrode material. Figure 12 of machined cast iron shows the recast phenomenon. Meanwhile machining of cemented tungsten carbide of Figure 13 shows the cracks and fragmentation trend. The fragmented particles implanted on the electrode surface and becomes as a new electrode tip.

Figure 13 shows the optical image of the accumulated solid material in the discharge gap which interrupt the machining process leads to random reading or stopping completely. The material is layered structure which is mean that it's related to the discharge sequence.

Scanning electron microscope: For further investigation SEM and EDX analyze are used. Figure 14 show the SEM image of the machined workpiece surface under experimental condition of EXP-1 shown in Table 3. Meanwhile, Fig. 15 is the SEM image of the machined surface under experimental condition of EXP-8 shown in Table 3.

Figure 14 is the SEM image of the machined cemented tungsten carbide machined at low Peak-Current, pulse duration and Gap-Voltage. It's clear that even at this low machining condition the crack is present. Figure 15 show the machined surface at higher Gap-Voltage and Peak-Current at constant pulse duration. It's clear that the surface damage is higher in EXP-8.

Figure16 shows SEM image of the accumulated solid material in the discharge gap. The material has a layered structure as mention before by optical image of Fig. 13. Each layer builds up from sub layers with an average thickness of submicron. The layered structure means that

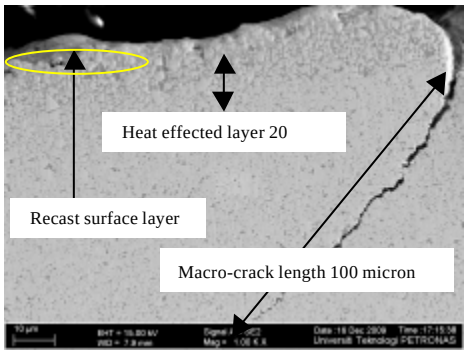

Fig. 14: Heat effected layer and crack penetration

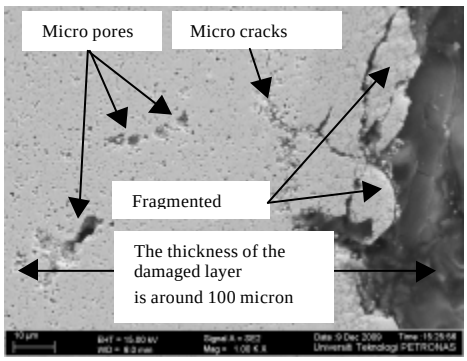

Fig. 15: The effect of surface cracks on surface finish

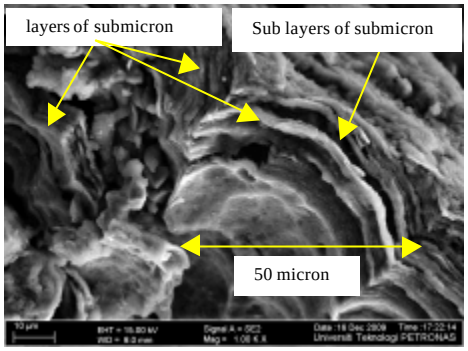

Fig. 16: The accumulated solid spongy material in the discharge gap

it's related to the discharge sequences. The structure of the surface is very effective during the application of this product. The effect of fracture behavior of cemented tungsten carbide during application also mentioned by Casas *et al*. (2006).

EDX analyses were carried out to analyze the chemical composition of this material. EDX profile was shown in Fig. 17. The result shows that the layers consist

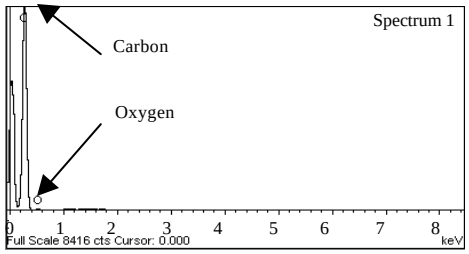

Fig. 17: EDX of the accumulated material in the gap

of carbon and oxygen and none of the electrode and workpiece composition detected inside these layers. The distances between the layers are not same which is mean that the discharge efficiency not stable.

CONCLUSION

The most effective variables on MRR, EW and Ra are gap voltage, Peak-Current, pulse ON-Time and pulse OFF-Time. The most effective variable on crack initiation is the discharge gap and peak current, respectively.

Gap-Voltage should be set at level lower than 150 volts to avoid any crack initiation at the early stage of marching, which leads to deeply cracks propagation and particles fragmentation.

It's found that at high peak current and gap voltage, the bigger fragmented particles implanted on the electrode surface and becomes as the new electrode tip resulting in changing of tool electrode material and geometry. As a consequence the machining process is not attaining the targeted output.

Generally high dielectric pressure is required to remove the debris and the broken up particles in the discharge gap.

Due to the low thermal conductivity, low thermal expansion and high heating rate, the high cooling rate is difficult to be achieved. This can create thermal stress higher than ultimate tensile strength which is the main source of cracks. It's recommended to use de ionized dielectric.

REFERENCES

Casas, B., Y. Torres and L. Llanes, 2006. Fracture and fatigue behavior of electrical-discharge machined cemented carbides. Int. J. Refractory Metals Hard Mater., 24: 162-167.

Jahan, M.P., Y.S. Wong and M. Rahman, 2009. A study on the fine-finish die-sinking micro-EDM of tungsten carbide using different electrode materials. J. Mater. Process. Technol., 209: 3956-3967.

Khan, A.A., M.E.B. Awang and A.A.B. Annuar, 2005. Surface roughness of carbides produced by abrasive water jet machining. J. Applied Sci., 5: 1757-1761.

Kiyak, M. and O. Cakir, 2007. Examination of machining parameters on surface roughness in EDM of tool steel. J. Mater. Proces. Technol., 191: 141-144.

Lee, S.H. and X. Li, 2003. Study of the surface integrity of the machined workpiece in the EDM of tungsten carbide. J. Mater. Process. Technol., 139: 315-321.

Lonardo, P.M. and A.A. Bruzzone, 1999. Effect of flushing and electrode material on die sinking EDM. CIRP Ann. Manuf. Technol., 48: 123-126.

Luis, C.J., I. Puertas and G. Villa, 2005. Material removal rate and electrode wear study on the edm of silicon carbide. J. Mat. Proces. Technol., 164-165: 889-896.

Puertas, I., C.J. Luis and L. Alvarez, 2004. Analysis of the influence of edm parameters on surface quality. MRR and EW of WC-Co. J. Mater. Proces. Technol., 153-154: 1026-1032.

Rahman, M.M., M.A.R. Khan, K. Kadirgama, M.M. Noor and R.A. Bakar, 2011. Experimental investigation into electrical discharge machining of stainless steel 304. J. Applied Sci., 11: 549-554.

Ratnasingam, J., T.P. Ma, G. Ramasamy and M. Manikam, 2009. The wear characteristics of cemented tungsten carbide tools in machining oil palm empty fruit bunch particleboard. J. Applied Sci., 9: 3397-3401.

Seghouani, M., A. Tafraoui and S. Lebaili, 2010. The damage of the cutting tools out of carbide metallic during the turning of a soaked and not hardened steel XC38. J. Applied Sci., 10: 813-822.

Upadhyasa, G.S., 1998. Cemented Tungsten Carbides Production, Properties and Testing. Noyes Publication, New York.

Xu, M.G., J.H. Zhang, Y. Li, Q.H. Zhang and S.F. Ren, 2009. Material removal mechanisms of cemented carbides machined by ultrasonic vibration assisted EDM in gas medium. J. Mater. Process. Technol., 209: 1742-1746.

Yang, K., B.S. El-Haik and B. El-Haik, 2009. Design for Six Sigma: A Roadmap for Product Development. 2nd Edn., McGraw-Hill Professional, USA.